



Online prediction of optimal deep brain stimulation contacts from local field potentials in Parkinson's disease



Marjolein Muller^{1,2}, Stefano Scafà^{3,4,5}, Ibrahem Hanafi⁶, Camille Varescon^{3,4}, Chiara Palmisano⁶,
Saskia van der Gaag², Rodi Zutt², Niels A. van der Gaag^{7,8,9}, Carel F. E. Hoffmann^{7,9}, Jocelyne Bloch^{4,10},
Mayte Castro Jiménez¹¹, Julien F. Bally¹¹, Philipp Capetian⁶, Ioannis U. Isaias^{6,12}, Eduardo M. Moraud^{3,4,13} &
M. Fiorella Contarino^{1,2,13}

Selecting optimal contacts for chronic deep-brain stimulation (DBS) requires a monopolar review, involving time-consuming manual testing by trained personnel, often causing patient discomfort. Neural biomarkers, such as local field potentials (LFP), could streamline this process. This study aimed to validate LFP recordings from chronically implanted neurostimulators for guiding clinical contact-level selection. We retrospectively analysed bipolar LFP recordings from Parkinson's disease patients across three centres (Netherlands: 68, Switzerland: 21, Germany: 32). Using beta-band power measures (13–35 Hz), we ranked channels based on clinical contact-level choices and developed two prediction algorithms: (i) a “decision tree” method for in-clinic use and (ii) a “pattern based” method for offline validation. The “decision tree” method achieved accuracies of 86.5% (NL), 86.7% (CH), and 75.0% (DE) for predicting the top two contact-levels. Both methods outperformed an existing algorithm. These findings suggest LFP-based approaches can enhance DBS programming efficiency, potentially reducing patient burden and clinical workload.

Deep brain stimulation (DBS) of the subthalamic nucleus (STN) is an effective treatment for Parkinson's disease (PD)^{1,2}. Optimisation of stimulation parameters is critical to maximise therapy efficacy. Identification of the optimal stimulation contact-level is challenging and time-consuming, requiring long iterative manual testing of multiple combinations (monopolar review, MPR), and several follow-up visits³. Novel neurostimulator devices are now capable of recording local field potentials (LFP) from the chronically implanted DBS electrodes, which may serve as a neural biomarker to guide clinical programming^{4–7}. LFP are generated by the integrated (weighted) sum of all synaptic potential changes⁸. These signals can

provide direct insight into the functioning of basal ganglia circuits^{8,9}. Subthalamic LFP activity within the beta-frequency band (13–35 Hz) correlates with akinetic-rigid symptoms in PD and can be modulated by therapies (e.g., levodopa and STN-DBS)¹⁰. Suppression of power in the beta-frequency band typically corresponds with motor improvement in PD patients.

To date, various studies have explored LFP-based DBS contact-level selection techniques, mostly relying on neural features in the beta-band¹¹. The maximum value of the beta-frequency power in a patient-specific range is mostly used as a measure to guide contact-level selection^{12–19}. However,

¹Department of Neurology, Leiden University Medical Center, Leiden, the Netherlands. ²Department of Neurology, Haga Teaching Hospital, The Hague, the Netherlands. ³Department of Clinical Neurosciences, University Hospital Lausanne (CHUV), Lausanne, Switzerland. ⁴Defitech Center for Interventional Neurotherapies (NeuroRestore), University Hospital Lausanne and Ecole Polytechnique Fédérale de Lausanne, Lausanne, Switzerland. ⁵Institute of Digital Technologies for Personalized Healthcare (MeDiTech), University of Applied Sciences and Arts of Southern Switzerland (SUPSI), Lugano, Switzerland. ⁶Department of Neurology, University Hospital of Wuerzburg and Julius Maximilian University of Wuerzburg, Wuerzburg, Germany. ⁷Department of Neurosurgery, Haga Teaching Hospital, The Hague, the Netherlands. ⁸Department of Neurosurgery, Leiden University Medical Center, Leiden, the Netherlands. ⁹University Neurosurgical Center Holland, Leiden University Medical Center, Haaglanden Medical Center and Haga Teaching Hospital, Leiden and The Hague, the Netherlands. ¹⁰Department of Neurosurgery, Lausanne University Hospital (CHUV) and University of Lausanne (UNIL), Lausanne, Switzerland. ¹¹Service of Neurology, Department of Clinical Neurosciences, Lausanne University Hospital (CHUV) and University of Lausanne (UNIL), Lausanne, Switzerland. ¹²Parkinson Institute of Milan, ASST G.Pini-CTO, Milan, Italy. ¹³These authors contributed equally: Eduardo M. Moraud, M. Fiorella Contarino.

e-mail: m.f.contarino@lumc.nl

Table 1 | Patient characteristics

	Training set "NL" (n = 34)	Validation set "CH" (n = 12)	Validation set "DE" (n = 16)	P value ^a
Age at surgery (years)	63.1 (SD 7.9)	64.4 (SD 6.0)	59.4 (SD 9.8)	0.321
Male, N (%)	23 (67.6%)	9 (75.0%)	14 (87.5%)	0.326
Disease duration at recording (years)	9.7 (SD 4.3)	9.1 (SD 2.8)	9.4 (SD 5.1)	0.807
Clinical total pre-operative OFF-med motor score	39.4 (SD 11.9)	39.7 (SD 11.4)	37.5 (SD 12.8)	0.846
Clinical total pre-operative ON-med motor score	18.9 (SD 9.1)	14.4 (SD 8.2)	14.1 (SD 7.0)	0.152
Levodopa response (OFF-ON/OFF*100)	52.6% (SD 17.5%)	66.1% (SD 15.8%)	63.4% (SD 12.0%)	0.030*
Preoperative LEDD	1350 (SD 591)	1112 (SD 583)	1100 (SD 466)	0.183
Time since lead implantation at LFP recording (days)	8.2 (SD 2.8)	5.6 (SD 1.5)	106.0 (SD 91.0)	<0.001*
Time since lead implantation at MPR (days)	9.2 (SD 1.1)	20.8 (SD 32.3)	106.6 (SD 20.2)	<0.001*

^aKruskal Wallis test (numerical data); Chi-square test (categorical data).

n number of patients, SD standard deviation, DBS deep brain stimulation, LEDD levodopa equivalent daily dose according to S.T. Jost et al.³⁷.

* Significant difference between groups (two-sided $p < 0.05$).

the clinical application of these techniques is still restricted due to limited validation, uncertainties regarding the reliability of the online visual inspection approach, or the need for complex methods and offline analysis. The most informative spectral feature of LFP for determining optimal stimulation therefore remains unclear.

Importantly, LFP activity is recorded bipolarly, between pairs of contact-levels. Identifying one individual monopolar stimulation level from these bipolar recordings presents a complex challenge. It has been suggested that either the contact-level in between the bipolar recording pair (e.g. contact-level 2 if channel (contact-level pair) 1–3 shows the highest maximum power) or one of the two recording contact-levels (e.g. contact-levels 1 or 3 if channel 1–3 shows the highest maximum power) could be the optimal stimulation location(s)^{18,19}. Studies addressing this issue using custom algorithms show a median predictive accuracy of 45% (range 25–71%) on selected datasets^{20–26}. However, these algorithms often focus on predicting an optimal horizontal direction for stimulation^{20–24} with directional leads, rather than an optimal vertical contact-level. Furthermore, they do not compare different predictors or techniques to derive monopolar predictions from bipolar recordings^{20–25}.

To better support initial DBS programming in PD, we explored the predictive efficacy of various beta-frequency band features using novel prediction techniques. We compared these novel techniques, which translate bipolar contact-level recordings to predictions for the optimal monopolar stimulation contact-level, with existing published algorithms.

Results

Subject characteristics

Across the three centres, a *BrainSense™ Survey* measurement (after overnight suspension of all dopaminergic drugs) was available for 62 patients (121 STN) (Table 1). Additionally, an extra set of patients ("CH", $N = 18$, 35 STN, of which 28 STN (80.0%) showed clear beta-activity) with recordings in ON-medication were included for a sub-analysis (Supplementary Table 1).

No chronic contact choice was available for 20 STN (17%). For the remaining 101 STN the contact-level used for chronic stimulation at 1 year (or 6 months if 1 year was not reached) post-lead placement differed from the contact-level chosen during MPR in 6 out of 58 STN (10%) for the "NL" dataset, in 3 out of 13 STN (23%) for the "CH" dataset, and in 8 out of 30 STN (27%) for the "DE" dataset (Supplementary Table 2). Of the 101 STN with a chronic contact choice, 83 STN showed clear beta activity.

Data pre-processing and feature extraction

No ECG or other definite artefacts were detected upon visual inspection in any of the datasets ("NL", "CH" and "DE"), therefore, no artefact extraction was applied.

Clear beta activity (based on "AUC_flat" threshold) was present in at least one recording channel for 80.5% of all leads (52/68 (76.5%) "NL"; 15/21

(71.5%) "CH"; 32/32 (100%) "DE"). The median value of AUC_flat was 2.64 (range: -2.81 to 13.60).

From clinically-chosen contact-level to recording channel ranking

For each clinically chosen contact-level individually, the amplitude of pre-determined features (Methods: "Data pre-processing and feature extraction"/"From clinically-chosen contact-level to recording channel ranking") was used to rank the recording channels. Rankings for the "Max" feature were similar to rankings obtained using the "AUC" feature. This similarity was also true for the "Max_flat" and "AUC_flat" rankings (Fig. 1 and Supplementary Fig. 1). Since the "Max" feature is most feasible for in-clinic use, we focus on this feature in the results.

The optimal contact-levels chosen by clinicians across our three centres highlighted that contact-levels 1 and 2 were most selected (35 and 53 hemispheres respectively), whereas contact-levels 0 and 3 were only seldom employed (4 and 7 hemispheres, respectively). The ranking of the LFP channels indicated that for contact-levels 1 and 2, the sensing channels surrounding the stimulation levels (i.e. 0–2 and 1–3), most often showed the highest feature amplitude (Fig. 1).

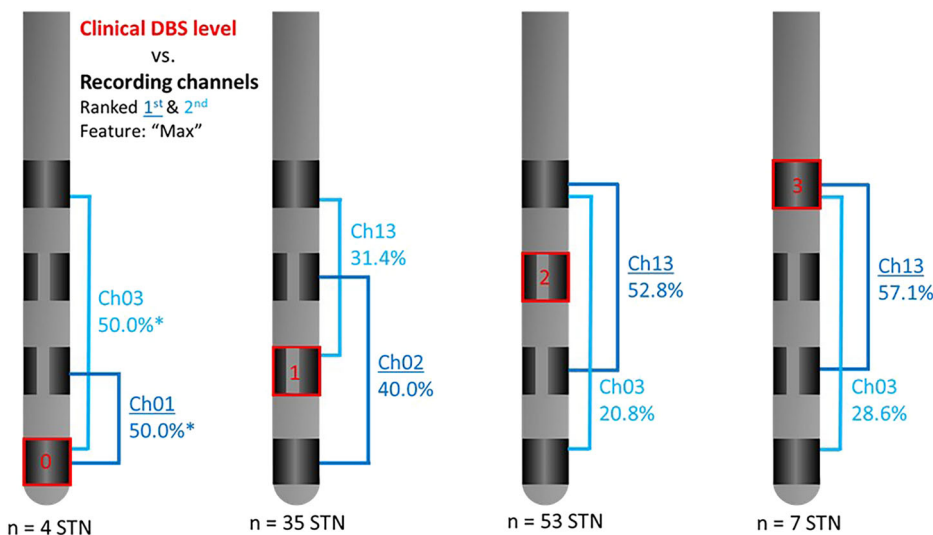
From recordings to contact-level prediction

We then evaluated the predictive accuracy of the 1st and 2nd ranked contact-levels defined by LFP, focusing on cases with clear beta activity across two custom prediction methods ("decision tree" and "pattern based" techniques) and one existing technique (DETEC algorithm), ("From recordings to contact-level prediction"). The "selection decision tree" method using the "Max" feature achieved 86.5% accuracy ("CH": 86.7%; "DE": 75.0%), increasing to 88.5% ("CH": 93.3%; "DE": 78.1%) when combining the selection and elimination trees (Fig. 2 and Supplementary Table 3). The "pattern based" method reached 84.6% accuracy ("CH": 66.7%, "DE": 71.9%) when considering both the 1st and 2nd ranked contact-levels.

Similar results were achieved when evaluating the chronically used stimulation level across 83 STN with available chronic contact-level data and clear beta activity using the "selection decision tree" with the "Max" feature ("NL": 83.7%; "CH": 90.0%; "DE": 86.7%). Clear beta activity was present in the 15 out of 17 STN with changes between chronic contact-levels and levels selected at MPR. For this subgroup, the predicted contact-level aligned with the clinically selected contact-level in 67.7% of the cases when considering the contact-level chosen at MPR, this agreement remained the same when considering the contact-level chosen at 1 year (or 6 months) post-operatively.

Both the "pattern based" and DETEC algorithms performed better when combining 1st and 2nd ranked contact-levels instead of considering the 1st ranked contact-level alone. However, the existing DETEC algorithm consistently showed lower predictive accuracies across all centres (Fig. 2 and

Fig. 1 | From clinically-chosen contact-level to recording channel ranking. This figure shows the first- (dark blue) and second-ranked (light blue) recording channel (Ch) per clinically chosen deep brain stimulation (DBS) contact-level at monopolar review (in red) for the maximal power beta-frequency band feature (“Max”). This shows how often the channel was ranked first based on this feature across the entire population of subthalamic nuclei (STN) as a percentage per 1st and 2nd ranked channel. Results shown are for all included leads with clear beta activity. (*) In case of an equal percentage (i.e., channels are ranked first with equal frequency) the channel which was ranked second most often, of these two options, was indicated as ranked 1st.



Supplementary Table 4). Similar results were observed when only focussing on the low-beta or high-beta bands for the “decision tree” and “pattern based” methods (Supplementary Table 5).

Analyses were repeated using the “Max_flat”, “AUC” and “AUC_flat” features for both the “decision tree” and “pattern based” methods. Changing the applied feature mostly resulted in minor differences in predictive accuracy. The “decision tree” method with both the selection and elimination tree in combination with the “AUC” feature achieved a slightly higher predictive accuracy in comparison to the “Max” feature for the “DE” dataset. The predictive accuracy across the “NL” and “CH” datasets was equal for both methods. When considering the “pattern based” method the “AUC_flat” feature slightly outperformed the use of the “Max” feature across the “NL” and “DE” datasets, and was equal for the “CH” dataset (Supplementary Tables 3, 4, and 6).

In order to evaluate the performance per clinically selected contact-level the accuracy of the “decision tree - selection tree only” using the “Max” feature and the “pattern based” model using the “AUC_flat” feature was additionally determined for each clinically selected contact-level separately across the entire population with clear beta activity. Both models showed accuracies above 70% for clinically selected contact-levels 0, 1 and 2, but not contact-level 3 (decision tree: 28.6%; pattern based: 57.1%), whereas the DETEC algorithm showed accuracies above 70% for clinically selected contact-levels 0 and 3, but not contact-levels 1 and 2 (level one: 52.9%; level two: 61.1%) (Supplementary Table 7).

Subgroup comparison

We then evaluated the predictive performance across hemispheres with little or no beta power above 1/f (Table 2). No significant differences were observed across any method or group. Across all data, containing all variations in beta-activity levels, the “decision tree” method, “pattern based” method and DETEC algorithm achieved predictive accuracies of 85.1%, 74.4% and 58.7%, respectively, when considering the 1st and 2nd ranked contact-levels.

A sub-analysis was performed for all “NL” recordings without clinically detectable stun effect during MPR (Table 3). Of the 26 STN with a stun effect, 11 (42.3%) also showed limited LFP-based beta activity (i.e. little beta above 1/3 or background activity only).

Patients with a stun effect had significantly lower predictive accuracy using the “pattern based” algorithm with the “Max” (if clear beta-activity) or “AUC” feature (if little beta-activity or background signals alone). The stun effect did not have a significant effect on the performance of the DETEC algorithm or “decision tree” method. No significant differences were found in patient characteristics, except for a

lower pre-operative OFF-medication motor score ($p = 0.029$) in the stun effect group (Supplementary Table 8).

Predictive accuracy differences between ON- and OFF-medication states were evaluated on an additional ON-medication “CH” dataset (Table 4). There were no significant differences in predictive accuracy or patient characteristics between subgroups (Supplementary Tables 1 and 9).

Discussion

We retrospectively evaluated LFP signals and their relation to clinically chosen stimulation contact-levels across three European centres and developed a novel algorithmic framework, including two complementary prediction algorithms, to identify optimal DBS contact-levels in over 60 PD patients.

The decision-tree approach using the “Max” feature showed high predictive accuracy (>85%) for the 1st and 2nd optimal contact-level predictions combined and showed robustness across validation sets. This new, online technique can thus help restrict the search field for optimal stimulation contacts to two contact-levels for the majority of patients, thereby showing the potential to reduce DBS programming time. Incorporating elimination trees improved results by 2 to 6 percental points, suggesting that this extra step might not be crucial and will only be reserved for selected cases.

The “pattern based” approach using the same feature correctly predicted the single optimal contact-level in 73.1% of the cases, and reached near 85% accuracy for combining 1st and 2nd optimal contact-level predictions. These results were, however, slightly less robust across validation sets compared to the online “decision tree” method.

Both approaches outperformed the existing DETEC algorithm for our datasets. However, we note that the predictive accuracy achieved by the DETEC-algorithm in the original research was higher than the predictive accuracy found on our data²⁰. The results from the “DE” dataset resemble the original results reported for the DETEC-algorithm most, likely because both datasets were recorded over 3 months post-lead placement.

Other existing algorithms using contact-level *BrainSense™ Survey* recordings (e.g.,²⁵) were not tested here, as they are not publicly available to our knowledge, and, based on the available literature, their accuracy is surpassed by the DETEC algorithm^{20,25}. Other existing algorithms are based on segmented *BrainSense™ Survey* recordings, which were not available in this retrospective analysis^{22–24,27}.

In all our analyses, using the “Max” and “AUC” feature yielded similar results. This indicates that albeit a single maximal value ignores the underlying PSD shape and is more prone to noise corruption, the conveyed information is enough for programming purposes. Once the aperiodic

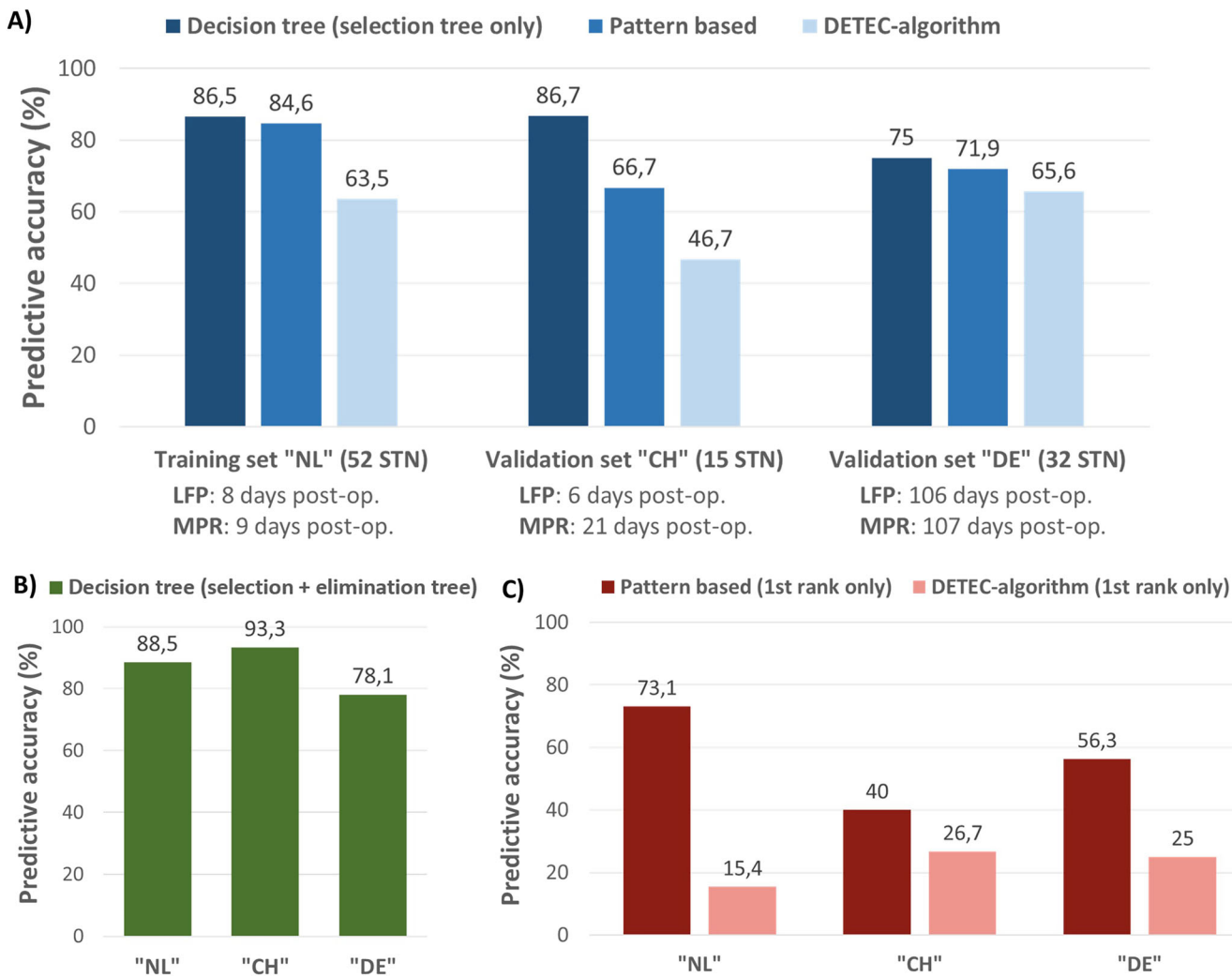


Fig. 2 | Comparison of the performance of the custom and existing algorithms. This figure shows a comparison of the predictive accuracy of the algorithms when considering the results for the 1st and 2nd ranked contact-levels in recordings with clear beta activity obtained in OFF-medication. The time from the implant to local field potential (LFP: used for prediction) and the time from implant to the clinical contact selection (monopolar review: reference for prediction) varied between centres (see text). A Predictive accuracy of the novel ‘decision tree –

selection only’ and ‘pattern based’ prediction techniques for the ‘Max’ beta feature in comparison to the predictive accuracy of the existing DETEC-algorithm when considering both the 1st and 2nd ranked contact-levels. **B** Predictive accuracy for the 1st and 2nd ranked contact-levels based on the online ‘decision tree’ method when applying the selection tree in combination with the elimination tree. **C** Predictive accuracy of the offline “pattern based” method and DETEC-algorithms for the 1st ranked contact-level alone.

Table 2 | Frequency of 1st/2nd ranked contact-levels corresponding to the clinically chosen stimulation level per ranking model for all patients from all three centres, subcategorised for clear or little beta above 1/f or background signal alone

	Decision tree ^a 1st / 2nd ranked	Pattern based 1st / 2nd ranked	DETEC algorithm 1st / 2nd ranked
Clear beta above 1/f ("NL": 52 STN, "CH": 15 STN, "DE": 32 STN)	“Max”: 82.8% (82)	“Max”: 77.8% (77)	61.6% (61)
Little beta above 1/f ("NL": 9 STN, "CH": 6 STN, "DE": 0 STN)	“AUC”: 93.3% (14)	“AUC”: 60.0% (9)	46.7% (7)
Background only ("NL": 7 STN, "CH": 0 STN, "DE": 0 STN)	“AUC”: 100.0% (7)	“AUC”: 57.1% (4)	42.9% (3)
Chi-square ^b	$\chi^2 = 2.434, p = 0.296$	$\chi^2 = 3.319, p = 0.190$	$\chi^2 = 1.968, p = 0.374$

Max maximum power feature, AUC area under the curve feature.

^aResults for selection decision tree only.

^bChi-square test was considered significant if two-sided $p < 0.05$.

Table 3 | Frequency of 1st/2nd ranked contact-levels corresponding to the clinically chosen stimulation level per ranking model for all “NL” patients, subcategorised as with/without stun effect

	Decision tree ^a – “Max/AUC” 1st / 2nd ranked	Pattern based – “Max/AUC” 1st / 2nd ranked	DETEC algorithm 1st / 2nd ranked
No stun (42 STN)	83.3% (35)	85.7% (36)	66.7% (28)
With stun (26 STN)	96.2% (25)	65.4% (17)	46.2% (12)
Chi-square ^b	$\chi^2 = 2.543, p = 0.111$	$\chi^2 = 3.860, p = 0.049$	$\chi^2 = 2.790, p = 0.095$

Max: maximum power feature.

^aResults for selection decision tree only.^bChi-square test was considered significant if two-sided $p < 0.05$.**Table 4 | Frequency of 1st/2nd ranked contact-levels corresponding to the clinically chosen stimulation level per ranking model for all “CH” patients, for the ON- versus OFF-medication state**

	Decision tree ^a - “Max” 1st / 2nd ranked	Pattern based – “Max” 1st / 2nd ranked	DETEC algorithm 1st / 2nd ranked
OFF-medication (21 STN)	85.7% (18)	66.7% (14)	47.6% (10)
ON- medication (35 STN)	71.4% (25)	68.6% (24)	51.4% (18)
Chi-square ^b	$\chi^2 = 1.503, p = 0.220$	$\chi^2 = 0.022, p = 0.883$	$\chi^2 = 0.076, p = 0.783$

Max maximum power feature.

^aResults for selection decision tree only.^bChi-square test was considered significant if two-sided $p < 0.05$.

signal component is removed, the channels ranked second changed to channels with a smaller pick-up area (e.g. for contact-level 2 channel 0–3 is ranked second using the “Max” feature, whereas channel 2–3 is ranked second using the “Max_flat” feature). These changes were similar for both the “Max” and “AUC” features. Furthermore, the ranking of the LFP channels indicated that for contact-levels 1 and 2, the sensing channels surrounding the stimulation levels (i.e. 0–2 and 1–3), most often showed the highest feature amplitude.

For the online “decision tree” method, the features without removal of 1/f outperformed the flattened features. This is very convenient, since visual inspection of a single point is easier and faster, especially in the context of clinical evaluations. However, the opposite was true for the offline “pattern based” method.

The performance of both the “decision tree” and “pattern based” methods generally showed greater variation between training and validation sets when features were applied after 1/f removal (“Max_flat”/“AUC_flat”) compared to when features were applied without it (“Max”/“AUC”). This suggests that results obtained using these features are more sensitive to variations between centres or patient groups, which can be considered a counterintuitive finding.

The presence of beta activity is often regarded as one of the limiting factors when considering beta power predictions. We thus clustered LFP recordings into subsets depending on their amount of beta power (clear beta-activity, little beta-activity, and background signal alone). While visually setting a threshold for minimal beta activity is inherently subjective, this approach aligns with clinical practice. Furthermore, no significant difference in performance was observed across the different levels of beta-activity for the proposed algorithms. Nonetheless, it is important to emphasise that the proposed methods depend on the presence of an electrophysiological biomarker, and that this limitation inherent to electrophysiology-based contact choice, restricts the applicability of these techniques across patients.

A second sub-analysis on the “NL” dataset alone showed that the performance of the “decision tree” method and DETEC-algorithm remained stable even in patients with a clinical stun effect during LFP recordings, whereas the performance decreased significantly for the “pattern based” method.

Across our three centres, the amount of AUC beta-activity without 1/f (“AUC_flat” feature) correlated with the time at which LFP recordings were performed. All the recordings with little beta activity or background signal alone were seen in the “NL” and “CH” datasets, for which LFP recordings were performed at an average of 8 and 6 days after implantation, respectively. The “DE” dataset, for which LFP recordings were performed at an average of 106 days after lead implantation, only contained LFP recordings with clear beta-activity.

In the “CH” ON-medication dataset, accuracy was similar with and without medication, opening up the possibility of avoiding overnight medication withdrawal in the future.

While both methods, especially the “decision tree”, were generally robust in different clinical and recording conditions, the “decision tree” method using the “Max” feature may be more reliable in the OFF-medication state and post-stun effect in individual patients. Adding the elimination tree could enhance prediction validity in selected cases, and further confirmation can be obtained using the “pattern based” method with the “AUC_flat” feature.

The studied population comprises a large cohort across three different centres, but limitations in the generalisation of the results should be considered. In the “NL” dataset, none of the STN were stimulated through contact-level 0, and only four (5.9%) through contact-level 3. This reflects the preferences and accuracy of the lead placement, as during surgery it is attempted to place the middle of the lead (contact-levels one and two, capable of steering) within the STN. This positioning is thereafter additionally confirmed using post-operative anatomical validation. This leads to contact-levels one and two being placed most optimally, explaining why these contact-levels are chosen for clinical stimulation with the highest frequency. Similar clinical selection patterns were seen in the other two datasets (“DE” level-0: 11.8%, level-3: 11.8%; “CH” level-0: 0.0%, level-3: 0.0%). Consequently, the evaluation of predictive techniques for contact-levels 0 and 3 was limited in reliability. Notably, contact-level 3 demonstrated the least favourable performance when assessed using the decision tree approach. However, it remains uncertain whether this reduced performance stems from the low sample size, clinical considerations such as a low threshold for side-effects at other contact-levels, or an actual decline in predictive accuracy for this level. Nonetheless, the correct identification of 6

out of 11 STNs at contact-levels 0 or 3 suggests that LFP-based contact selection may still offer valuable guidance and reduce programming time more effectively than defaulting to contact-levels 1 and 2 alone.

Additionally, although no artefacts were visually identified, there may have been artefacts overlapping with the neurophysiological signal may have been present. Furthermore, differences in impedances between recording channels were not considered. Similarly, variations in distances between recording levels were not directly corrected in the new techniques, unlike the DETEC-algorithm. However, these distance variations were indirectly addressed through averaging in the “pattern based” method and through specific branch designs in the “decision tree” method.

The developed methods were not assessed for identifying the optimal stimulation segment in directional contacts, as segmented *BrainSense™ Survey* recordings were unavailable for most patients. By contrast, other algorithms, such as the DETEC algorithm, often support optimal segment identification. Nonetheless, the choice of directionality forms a second step in identifying the optimal stimulation, and is not needed in many individuals at the time of MPR²⁸. At this time our methods do not include directionality, but do enable a fast choice among the available contact-levels, without the need for longer, additional segmented *BrainSense™ Survey* recordings.

Another important point is that bipolar recordings reflect the difference in electrical activity between two recording points, making direct translation to a single location with the highest activity inherently complex. Crucially, our work represents one of several efforts to propose a viable method for translating bipolar recordings to monopolar contact-level selection. However, such translations will inherently involve some degree of estimation. The future availability of (pseudo)monopolar LFP recordings may enhance prediction accuracy by removing the need for bipolar-to-monopolar translation, although this shift may introduce new challenges for implanted systems. Despite these advancements, bipolar recordings will remain essential during therapeutic stimulation and are likely to continue playing a pivotal role in the development of future adaptive systems.

We evaluated beta-based features within the 13–35 Hz range, which differs from the beta range shown by the clinician programmer (8–30 Hz). Additionally, a distinction between low- and high-beta activity was not made for all analyses, as initial results showed no clear difference in predictive accuracy. Furthermore, not all patients exhibit a clear separation between low- and high-beta peak, as many patients showed a single peak around 20–21 Hz. In these cases separating low- and high-beta bands would artificially lead to two “Max” and “Max_flat” features, biasing the results. Moreover, several patients only showed either low- or high-beta peaks but not both. This further illustrates that the distinction between low- and high-beta can be very complex and that specifically developing an algorithm for the individual low- or high-beta band would complicate the clinical workflow and reduce the clinical applicability. In this study we focussed mainly on the full beta-band, aiming to develop a simple and robust method that can be readily implemented in clinical practice. However, not all patients show a distinct relation between beta suppression and motor improvement^{29–31}. Moreover, features from other frequencies may aid in predicting optimal stimulation levels^{13,32–34}.

After MPR, the contact-level for chronic stimulation is typically selected based on the lowest threshold for therapeutic benefit, while also considering the absence of side-effects. This implies that even if a contact has the lowest threshold for benefit, it might still be excluded due to the presence of side-effects—an aspect that may not be fully reflected by LFP measurements. In this retrospective study, we were unable to verify this, as some necessary data were unavailable.

Additionally, if a stun effect occurs during MPR, the clinical contact level might be chosen based on other considerations, such as anatomical factors, personal preferences of the physician. Selecting a contact based on these other alternative factors could potentially lead to a choice that is suboptimal for stimulation. To correct for this, we also considered the contact-level used for stimulation 6–12 months after implant and found few differences (in 9–13 STN, ≤ 25%). Finally, even though the Percept PC®

sensing capabilities were programmatically not used to select the most optimal contact-level during clinical programming, we cannot guarantee that physicians were blinded to the results of the sensing due to the retrospective character of the study. However, the fact that across all STN 86% of the contacts selected for chronic stimulation remained unchanged after 6–12 months further confirms that the clinical contact-level choice during MPR was indeed clinically optimal.

This study introduces and validates both online and offline tools for supporting selection of optimal clinical contact-levels, potentially reducing the time required for the initial optimal contact-level selection. The presented novel approaches are robust under varying clinical conditions. The online decision tree is particularly practical for clinical use.

Future research should explore including directionality using the segmented *BrainSense™ Survey* recordings, and should consider incorporating features from other frequency bands, which may relate to certain PD symptoms and/or disease states³⁵. In addition, integrating our methods with imaging data could provide information on the expected locations of side-effects. Including information on stimulation-induced beta-suppression could further enhance optimal contact-level selection^{21,23}. Future availability of monopolar LFP recordings might also improve predictions by eliminating the need for a bipolar to monopolar translation, although new challenges may arise in implanted systems.

While the proposed methods can enhance LFP-based contact-level selection and reduce testing time, especially in case of clinical complexity, clinical judgement and case-by-case considerations should always remain.

Methods

Study design

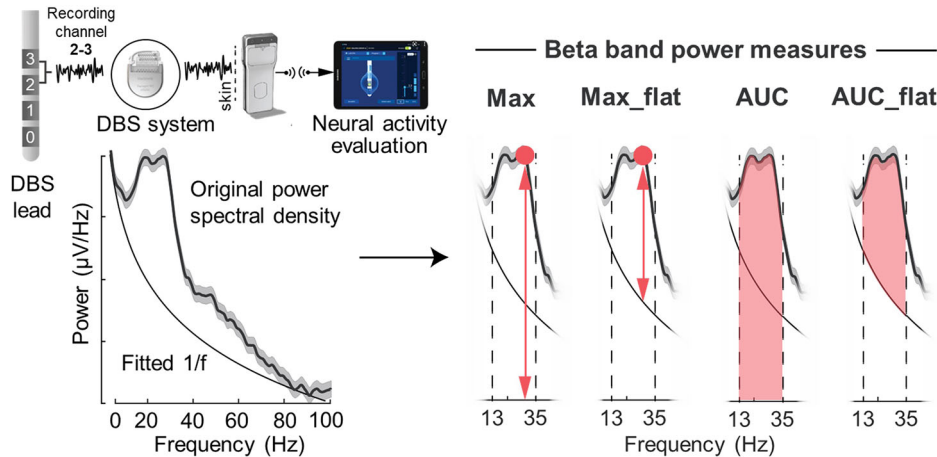
This study concerns a retrospective, international multi-centre study across three DBS centres: Haga Teaching Hospital/Leiden University Medical Centre (The Netherlands (NL)); Lausanne University Hospital, (Switzerland (CH)); University Hospital of Würzburg (Germany (DE)). In the three participating centres, PD patients implanted in the STN with directional Sensight™ leads in combination with the Percept PC® neurostimulator (Medtronic, Minneapolis) were screened for inclusion. The Medical ethical committee Leiden-Den Haag-Delft (reference N23.007), the local Ethical Committee of the University of Würzburg (reference n. 103/20-am) and the Ethics Committee of the Canton de Vaud, Switzerland (reference PB_2017-00064) approved the respective studies and/or waived review for the data collection of the respective centre. All patients gave written informed consent or consent was obtained through an opt-out procedure for the reuse of routinely recorded health data for scientific research as approved by the ethics committee, according to the Declaration of Helsinki.

Data acquisition

Contact-level bipolar LFP recordings conducted in the OFF-medication state (i.e. after overnight suspension of all dopaminergic drugs) with the *BrainSense™ Survey* were used. The *BrainSense™ Survey* enables 90-s in-clinic recordings with stimulation OFF, capturing ~21 s of LFP power spectra per contact pair online, plus raw time-domain data (250 Hz) for offline analysis. This research focussed on contact-level recordings (rings 0 and 3 and virtual rings 1abc and 2abc, each composed of 3 independent segments) of the directional Sensight™ lead, and did not evaluate individual segments (1a,-b,-c or 2a,-b,-c). All “NL” and “CH” recordings were performed within the first two weeks after lead implantation without previous DBS therapy, whereas “DE” measurements were mostly collected after a longer follow-up with a stimulation washout period of approximately 3 h prior to MPR.

The contact-level chosen for chronic stimulation by the clinician after MPR served as a reference for all the LFP-based predictions. MPR was performed according to the clinical standard protocol (≥12 h OFF-medication), evaluation of side-effects and selected UPDRS-III scores at each contact level using small incremental increases in stimulation amplitude, between 8 days and 3 months after lead implantation. For all centres, we additionally compared the level of the electrodes used for chronic

Fig. 3 | Feature extraction method. This figure demonstrates the use of the original spectrum and FOOOF-algorithm aperiodic fit for the extraction of four beta-band power measures: the maximum power (Max); the maximum flattened (i.e. after removal of the aperiodic signal component) power (Max_flat); the area under the curve (AUC); and the flattened area under the curve (AUC_flat).



stimulation at 1 year after surgery. In the case of interleaved programming at follow-up, we considered the contact with the highest stimulation amplitude, or, in the case of an equal contribution by both contacts, the contact with the smallest distance to the contact chosen at MPR. If directional stimulation was applied at follow-up the contact-level containing the active segment was considered.

Data pre-processing and feature extraction

Matlab (version R2022b, MathWorks®) was used for all data pre-processing and analyses.

Available *Brainsense™ Survey* measurements were visually inspected for potential artefacts in the frequency and time domain. For the analyses, the frequency and power data derived from the time-to-frequency conversion embedded in the Percept PC® neurostimulator were used. Feature power values were thereafter determined by means of a custom Matlab script (<https://doi.org/10.17605/OSF.IO/FZN8D>). All analyses were performed for the left and right hemispheres separately. Stimulation contact-levels for both hemispheres were numbered 0, 1, 2 and 3 (ventral, ventromedial, dorsomedial, dorsal). When using the *Brainsense™ Survey* measurement bipolar recordings are conducted for the following six channels (contact-level pairs): 0–1; 0–2; 0–3; 1–2; 1–3; 2–3.

From all recording channels, four features of the beta-frequency band (13–35 Hz) were extracted. The first is the maximum beta power value (“Max”), commonly used in clinical practice, as it is easily readable from the clinician programmer’s screen. To account for varying background noise across contacts, we also assessed this feature after removing the 1/f component (“Max_flat”) using the FOOOF algorithm (v1.0.0 with MATLAB wrapper v1.0.0), which decomposes the 1–100 Hz power spectrum into aperiodic and periodic components via parametric curve fitting, optimising the modelled spectrum with a least-squared-error approach³⁶. The third feature was the area under the curve over the whole beta-frequency band (“AUC”), which may be more representative or stable than a simple discrete value but requires offline analysis. This feature was additionally evaluated after removing the aperiodic 1/f component (“AUC_flat”) (Fig. 3). For the main analyses, only *Brainsense™ Survey* recordings with a detectable beta-peak were included. The presence of the beta-peak was determined using a threshold for the “AUC_flat” value. In secondary analyses, the impact of limited beta-activity on the predictive accuracy of the proposed techniques was further assessed. Furthermore, in the subset of “NL” patients we evaluated the predictive accuracy of the techniques when individually focussing on the low-beta (13–20 Hz) or high-beta (21–35 Hz) peak activity (“Max” feature).

From clinically-chosen contact-level to recording channel ranking

We aimed to determine the relation between bipolar recordings and clinical choice. To this end, for each clinically chosen contact-level across all

hemispheres, we ranked all LFP recording channels based on the amplitude of each of the four aforementioned features individually (Fig. 1 and Supplementary Fig. 1).

From recordings to contact-level prediction

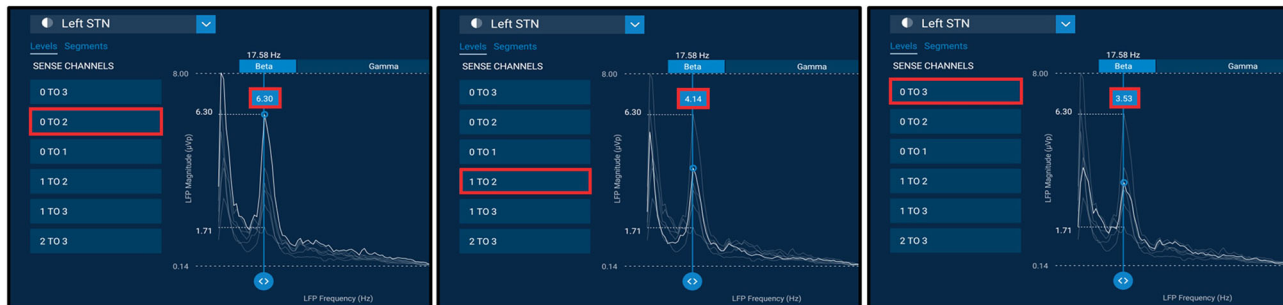
To test the possibility of predicting the clinically-chosen contact-level directly from LFP recordings, two custom ranking methods were developed and evaluated, together with an existing ranking model (DETEC-algorithm²⁰). All “NL” recordings were used to design the ranking methods (training set). External validation was performed using the “CH” and “DE” datasets (validation sets).

The first custom ranking method, the “decision tree” method involves a decision tree set of hierarchical models. This method was developed as a tool to be used for online, in-clinic applications. The applied method is based on the physical principle that strong beta power observed between contact pairs results from a large difference in beta-power between these contact-levels. A high difference in beta-power indicates that one contact-level is very close, while the other is expected to be relatively far from the beta-source (i.e., sweet spot), for example inside or outside the motor part of the STN. By analysing which pairs and locations across the lead show the strongest beta activity, we can infer which individual contact-levels are located closest to the beta source. Based on this principle the decision tree is sequentially navigated using the channels with the first, second, and, when applicable, third highest feature values. The additional third step in the tree applies mostly when the second highest feature value leads to a channel with a large intercontact distance. By doing so the method accounts for differences in intercontact distance.

There are two types of decision trees, a “selection tree” and an “elimination tree”, which can be applied consecutively. The “selection tree” uses the three bipolar recordings with the highest beta-peak (“Max” feature) to select the two best stimulation contact-levels (Fig. 4 and Supplementary Fig. 2). The two best contact-levels are always assumed to be adjacent levels (i.e. 0&1 or 1&2 or 2&3), as we expect a single beta-source. Contact-levels at the top (2&3) or bottom (0&1) of the lead are selected when the highest difference in beta power occurs in channels surrounding the middle 2 contact-levels of the lead (i.e. 0–2, 1–3, 0–3), followed by channels located at the top or bottom of the lead (i.e. 0–1 or 2–3), as this indicates that the beta-source is either at the top or bottom of the lead. For instance, if the highest feature value is present in channel 1–3, followed by channel 0–3, the strongest beta-power can be located at the top (3) or bottom (0/1) of the lead. If the third highest feature value is then located in channel 2–3 we expect the strongest beta power to be located in the contact-levels at the top of the lead (2&3), as opposed to the bottom contact-levels (0&1) (see different example in Fig. 4).

Contact-levels at the middle of the lead (1&2) are selected when the highest difference in beta power occurs most in channels surrounding the middle 2 contact-levels of the lead (i.e. 0–2, 1–3, 0–3), followed by channels located at the middle of the lead (i.e. 1–2), as this indicates that the beta-

A Clinician programmer results



B Corresponding “Decision tree” results

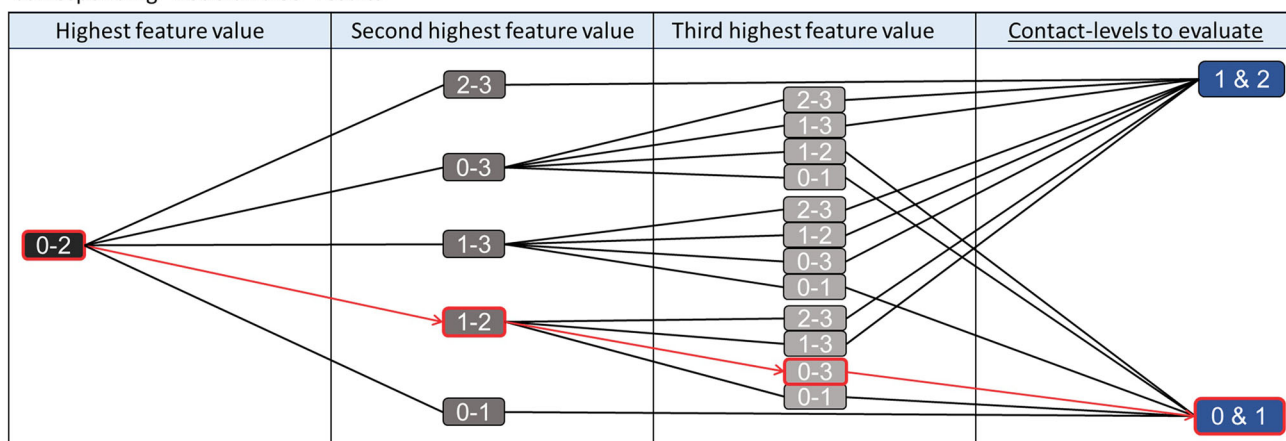


Fig. 4 | The “decision tree” ranking method. This figure shows an example of the “selection decision tree” online ranking technique which uses the two or three recording channels with the highest beta feature value to select the two most likely best contact-levels. **A** For this method the clinician performs a BrainSense™ Survey for the contact-levels using the clinician programmer. These contact-level recordings can thereafter be used on-screen to visually select the channel (contact pair) with the highest beta peak (i.e. channel “0 to 2” in this example). **B** This information is used to choose the appropriate “selection decision tree”, i.e. the one which starts with the selected channel. Hereafter, the channel with the second highest beta peak (here

channel “1 to 2”) is selected in the first branch of the decision tree. Finally, the channel with the third highest beta peak (here channel “0 to 3”) is selected in the second and final branch. The final block highlights the most promising contact-levels, identified here as levels 0 and 1. The large power between contact pairs 0–2 and 1–2 (highest and second-highest) could be due to either high power on contact 2 (and low on 0 and 1), or high power on contacts 0 and 1 (and low on 2). Because the third highest power is on contact pairs 0–3, this indicates that the large power is on 0 (and thus not on 2), only leaving out 0 and 1. These conclusions are derived using the “selection decision tree” technique only.

source is most likely at the middle of the lead. For instance, if the highest feature value is present in channel 1–3, followed by channel 0–2, the strongest beta power can be located anywhere across the lead. If this is then followed by channel 1–2, we expect the strongest beta power to be located at the middle contact-levels (1&2).

As a second step the “elimination tree” can help discard the least promising stimulation levels by looking at the bipolar recordings with the lowest beta-peak (Supplementary Fig. 3). The same principles apply as with the “selection tree”, but contact-levels can only be eliminated when it is certain they are not part of the beta-source. As a result, sometimes only one contact-level is eliminated instead of two. For example, if the lowest beta power difference is observed in channel 1–3, followed by 0–3, the lowest beta power is likely at the top (3) or bottom (0/1) of the lead. If channel 0–1 follows with the third lowest beta power, both assumptions are probably correct, and contact-levels 0 and 3 can be eliminated. However, if channel 1–2 follows, we cannot exclude the possibility that the bottom of the lead (0/1) is part of the beta-source, so only contact-level 3 can be eliminated.

We tested whether the use of the elimination tree in addition to the selection tree increased the accuracy. This online selection technique was additionally tested for the three remaining features (AUC, Max_flat and AUC_flat). However, results relying on the “Max” feature are considered of greatest value as this method is most viable in an online clinical setting.

The second custom ranking method, the “pattern based” method, involves a non-iterative method that maps the distribution of beta features across all bipolar recording pairs and provides an estimate of

relevance for all stimulation contact candidates (<https://doi.org/10.17605/OSF.IO/FZN8D>). Albeit more computationally expensive, this “pattern based” process allows offline confirmation of the choice derived from the online decision-tree approach. Contributions to each stimulation contact may come from bipolar combinations that include the contact, as well as from pairs that surround the contact, our approach inherently accounts for both. Additionally, this method partially compensates for variations in intercontact distance by averaging across all distances and subsequently comparing results between contact-levels that share the same (average) distance.

In this “pattern based” method, beta features of all channels are first mapped onto a heatmap to represent the spatial distribution of the beta feature and the relative power that each bipolar recording channel conveys. This heatmap can then be used to derive the overall contribution of beta power to each contact-level by combining two methods. Method 1: averages the feature value across all channels which include the contact (e.g. for level 0: channel 0–1, channel 0–2 and channel 0–3); method 2: evaluates the feature value of the channels surrounding level 1 and 2 (e.g. for level 1: channel 0–2). The maximum value from both methods is kept, and the contact-level with the highest feature value is selected as the optimal DBS contact-level (Fig. 5).

We aimed to compare the results of both the online and offline developed custom ranking methods to existing algorithms. As we only had access to level-based *Brainsense™ Survey* recordings, the only published

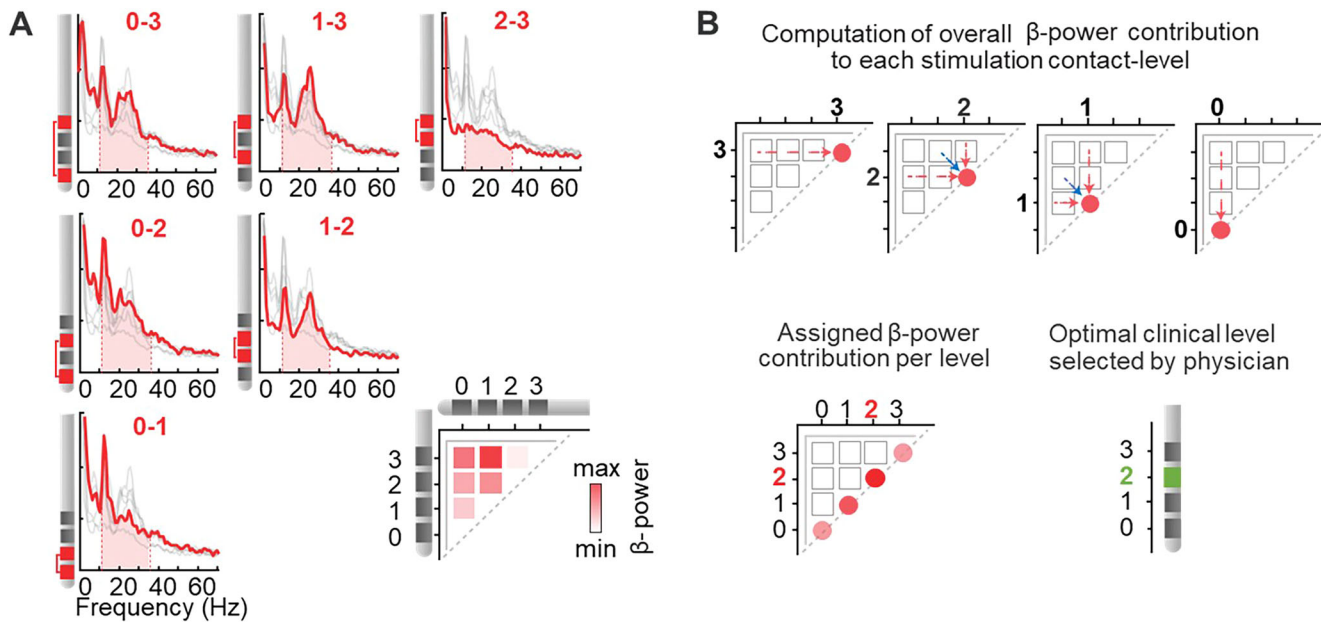


Fig. 5 | The “pattern based” ranking method. This figure shows an example for the “pattern based” ranking technique which computes a single feature value per eligible contact-level to use for the selection of the optimal stimulation level. **A** The feature value (example in figure = area under the curve (AUC)) is determined for all recording channels (contact pairs) on one lead. This information is thereafter summarised in a single image where the intersection of contact-levels is represented on two axes using a heatmap with colour intensity corresponding to the feature value. (In this example maximum AUC power was at contact pairs 1–3 and minimum at contact pairs 2–3). **B** The information in the summary image is thereafter converted using the “pattern based” method to provide a single “beta-power contribution” value for each of the four eligible contact-levels. This conversion is performed by: (1) averaging all feature values

for channels including a certain level and assigning this value to the respective contact-level (e.g. for level 0 feature values of: channel 0–1, channel 0–2 and channel 0–3 – red arrows – are averaged to obtain a single “beta-power contribution” value for level 0), and (2) in addition, for contact levels 1 and 2, the feature power of the contact pairs adjacent to these levels (e.g. for level 1: channel 0–2, blue arrows) is compared to the values obtained in step (1) and the highest value between the two is assigned to these contact levels. This result is stored in a single “beta-power contribution” value per eligible contact-level. The level with the highest assigned value is then considered as the predicted optimal level (Here: level 2). This prediction can then be compared to the optimal clinical level selected by the physician (green in the figure) to determine the predictive accuracy of the “pattern based” technique.

algorithm that could be included was the DETEC-algorithm (Eq. 1), which is an offline algorithm²⁰.

$$\text{PSD}_{\text{weighted}} = \frac{\sum_{i=1}^n \text{PSD}_i * \frac{1}{d_i}}{\sum_{i=1}^n \frac{1}{d_i}} \quad (1)$$

In Eq.(1), PSD_i is the power spectral density from bipolar recording i of the n bipolar recordings involving the investigated contact-level. d_i is the distance between the centre of the investigated contact-level and its bipolar recording partner for each i -th bipolar recording (mm).

Model evaluation

To assess each ranking model’s performance, we calculated how often the clinically chosen stimulation level matched the 1st ranked contact-level, or the 1st or 2nd ranked level (without any priority/weight), based on LFP. Including both the 1st and 2nd ranked levels allowed fair comparison between the “decision tree” method, which often selects two optimal contact-levels, and the other models, where a single optimal contact-level can be selected.

Ranking models were additionally evaluated for sub-groups based on their amount of AUC beta activity without $1/f$ (“AUC_flat” feature). Visual inspection defined that below a threshold of $0.6\mu\text{V}$, the detection of a beta-peak was unclear. We thus clustered hemispheres into the following three groups: (i) “clear beta”: at least one channel with “AUC_flat” $\geq 0.6\mu\text{V}$. (ii) “little beta”: one or more channels with “AUC_flat” between 0.0 and $0.6\mu\text{V}$. (iii) “background signal only”: all channels with “AUC_flat” $\leq 0.0\mu\text{V}$. Even in cases with a flattened power (“little beta” or “background signal only”), we could still extract an order from the global beta (i.e., background activity in the beta-band) (Supplementary Fig. 4). Therefore, ranking

using the “AUC” feature is still possible in these cases, providing similar results as visual ranking of background activity in clinical practice.

For the “NL” dataset, ranking models were evaluated for a subgroup of hemispheres with a stun effect at the time of MPR. A stun effect was considered when the symptoms were too mild to allow a reliable clinical evaluation at MPR (MDS-UPDRS-III OFF-medication score for bradykinesia, rigidity and tremor equal to 0 or 1).

The predictive accuracy of the algorithms was also assessed for a subset of LFP recordings (“CH” ON) where patients were ON-medication (i.e. practically defined ON).

Statistical analysis

Differences in population characteristics were evaluated using a Kruskal-Wallis test for numerical data or a Chi-Square test in case of categorical data. A Chi-square test was used to investigate significant differences in performance based on the subgroups described in 2.4.1–2.4.3. In all statistical evaluations, a two-sided p -value smaller than 0.05 was considered significant.

Data availability

The datasets used and analysed during the current study available from the corresponding author on reasonable request.

Code availability

The underlying code for this study is available in the Open Science Framework and can be accessed via <https://doi.org/10.17605/OSF.IO/FZN8D>.

Received: 26 November 2024; Accepted: 23 July 2025;

Published online: 08 August 2025

References

1. Ince, N. F. et al. Selection of optimal programming contacts based on local field potential recordings from subthalamic nucleus in patients with Parkinson's disease. *Neurosurgery* **67**, 390–397 (2010).
2. Pintér, D. et al. Antiparkinsonian drug reduction after directional versus omnidirectional bilateral subthalamic deep brain stimulation. *Neuromodulation* **26**, 374–381 (2023).
3. Volkmann, J., Moro, E. & Pahwa, R. Basic algorithms for the programming of deep brain stimulation in Parkinson's disease. *Mov. Disord.* **21**, S284–S289 (2006).
4. Medtronic. PERCEPT PC-NEUROSTIMULATOR medtronic.eu20202020 [Available from: <https://europe.medtronic.com/xd-en/healthcare-professionals/products/neurological/deep-brain-stimulation-systems/percept-pc.html>].
5. Isaias, I. U. et al. Case report: Improvement of gait with adaptive deep brain stimulation in a patient with Parkinson's disease. *Front. Bioeng. Biotechnol.* **12**, 1428189 (2024).
6. Caffi, L. et al. Adaptive vs. conventional deep brain stimulation: one-year subthalamic recordings and clinical monitoring in a patient with Parkinson's Disease. *Bioengineering* **11**, 990 (2024).
7. Arlotti, M. et al. Monitoring subthalamic oscillations for 24 h in a freely moving Parkinson's disease patient. *Mov. Disord.* **34**, 757–759 (2019).
8. Lashgari, R. et al. Response properties of local field potentials and neighboring single neurons in awake primary visual cortex. *J. Neurosci.* **32**, 11396–11413 (2012).
9. Einevoll, G. T., Kayser, C., Logothetis, N. K. & Panzeri, S. Modelling and analysis of local field potentials for studying the function of cortical circuits. *Nat. Rev. Neurosci.* **14**, 770–785 (2013).
10. Brittain, J.-S. & Brown, P. Oscillations and the basal ganglia: motor control and beyond. *NeuroImage* **85**, 637–647 (2014).
11. van Wijk, B. C. M., de Bie, R. M. A. & Beudel, M. A systematic review of local field potential biomarkers in Parkinson's disease: from clinical correlations to adaptive deep brain stimulation algorithms. *J. Neurol.* **270**, 1162–1177 (2023).
12. Xu, S. S. et al. Can brain signals and anatomy refine contact choice for deep brain stimulation in Parkinson's disease? *J Neurol Neurosurg Psychiatry* **93**, 1338–1341 (2022).
13. Xu, S. S. et al. Towards guided and automated programming of subthalamic area stimulation in Parkinson's disease. *Brain Commun.* **4**, fcac003 (2022).
14. Sinclair, N. C. et al. Electrically evoked and spontaneous neural activity in the subthalamic nucleus under general anesthesia. *J Neurosurg.* **137**, 449–458 (2021).
15. Milosevic, L. et al. Online mapping with the deep brain stimulation lead: a novel targeting tool in Parkinson's disease. *Mov. Disord.* **35**, 1574–1586 (2020).
16. Tamir, I. et al. Eight cylindrical contact lead recordings in the subthalamic region localize beta oscillations source to the dorsal STN. *Neurobiol. Dis.* **146**, 105090 (2020).
17. Tinkhauser, G. et al. Directional local field potentials: a tool to optimize deep brain stimulation. *Mov. Disord.* **33**, 159–164 (2018).
18. Kochanski, R. B., Shils, J., Verhagen Metman, L., Pal, G. & Sani, S. Analysis of movement-related beta oscillations in the off-medication state during subthalamic nucleus deep brain stimulation surgery. *J. Clin. Neurophysiol.* **36**, 67–73 (2019).
19. Thenaisie, Y. et al. Towards adaptive deep brain stimulation: clinical and technical notes on a novel commercial device for chronic brain sensing. *J. Neural Eng.* **18**, 042002 (2021).
20. Strelow, J. N. et al. Local field potential-guided contact selection using chronically implanted sensing devices for deep brain stimulation in Parkinson's Disease. *Brain Sci.* **12**, 1726 (2022).
21. Strelow, J. N. et al. Low beta-band suppression as a tool for DBS contact selection for akinetic-rigid symptoms in Parkinson's disease. *Parkinsonism Relat. Disord.* **112**, 105478 (2023).
22. Binder, T. et al. Feasibility of local field potential-guided programming for deep brain stimulation in Parkinson's disease: A comparison with clinical and neuro-imaging guided approaches in a randomized, controlled pilot trial. *Brain Stimul.* **16**, 1243–1251 (2023).
23. Busch, J. L. et al. Local field potentials predict motor performance in deep brain stimulation for Parkinson's Disease. *Mov. Disord.* **12**, 1726 (2023).
24. di Biase, L. et al. Intraoperative local field potential beta power and three-dimensional neuroimaging mapping predict long-term clinical response to deep brain stimulation in Parkinson Disease: a retrospective study. *Neuromodulation* **26**, 1724–1732 (2023).
25. Lewis, S. et al. Pilot study to investigate the use of in-clinic sensing to identify optimal stimulation parameters for deep brain stimulation therapy in Parkinson's Disease. *Neuromodulation* **27**, 509–519 (2023).
26. Dong, W. et al. The guiding effect of local field potential during deep brain stimulation surgery for programming in Parkinson's disease patients. *CNS Neurosci. Ther.* **30**, e14501 (2023).
27. Niso, G. et al. Brainstorm pipeline analysis of resting-state data from the open MEG archive. *Front. Neurosci.* **13**, 284 (2019).
28. Zitman, F. M. P. et al. The actual use of directional steering and shorter pulse width in selected patients undergoing deep brain stimulation. *Parkinsonism Relat. Disord.* **93**, 58–61 (2021).
29. Ozturk, M. et al. Distinct subthalamic coupling in the ON state describes motor performance in Parkinson's disease. *Mov. Disord.* **35**, 91–100 (2020).
30. Kühn, A. A. et al. Pathological synchronisation in the subthalamic nucleus of patients with Parkinson's disease relates to both bradykinesia and rigidity. *Exp. Neurol.* **215**, 380–387 (2009).
31. Hill, M. E. et al. Paradoxical modulation of STN β-Band activity with medication compared to deep brain stimulation. *Mov. Disord.* **39**, 192–197 (2024).
32. Nguyen, T. A. K., Schüpbach, M., Mercanzini, A., Dransart, A. & Pollo, C. Directional local field potentials in the subthalamic nucleus during deep brain implantation of Parkinson's disease patients. *Front. Hum. Neurosci.* **14**, 521282 (2020).
33. Connolly, A. T. et al. eds. Guiding deep brain stimulation contact selection using local field potentials sensed by a chronically implanted device in Parkinson's disease patients. In *2015 7th International IEEE/EMBS Conference on Neural Engineering (NER)* (IEEE, 2015).
34. Shah, A. et al. Combining multimodal biomarkers to guide deep brain stimulation programming in Parkinson Disease. *Neuromodulation* **26**, 320–332 (2023).
35. Yin, Z. et al. Local field potentials in Parkinson's disease: a frequency-based review. *Neurobiol. Dis.* **155**, 105372 (2021).
36. Donoghue, T. et al. Parameterizing neural power spectra into periodic and aperiodic components. *Nat. Neurosci.* **23**, 1655–1665 (2020).
37. Jost, S. T. et al. Levodopa dose equivalency in Parkinson's disease: updated systematic review and proposals. *Mov. Disord.* **38**, 1236–1252 (2023).

Acknowledgements

The authors are thankful to Prof. dr ir. A.C. Schouten and his team for helpful insights. M.M. and M.F.C. were supported by the European Union's Horizon Europe research and innovation programme under grant agreement number 101070865 (MINIGRAPH). C.P. was supported by the Deutsche Forschungsgemeinschaft (DFG, German Research Foundation) Project-ID 424778381 - TRR 295, and the Fondazione Europea per la Ricerca Biomedica (FERB). IH was supported by a scholarship from the German Academic Exchange Service (DAAD; Deutscher Akademischer Austauschdienst). IUI was supported by the Fondazione Pezzoli per la Malattia di Parkinson, from the New York University School of Medicine and the Marlene and Paolo Fresco Institute for Parkinson's and Movement Disorders, which was made possible with support from Marlene and Paolo Fresco, and by the European Union—Next Generation EU—NRRP M6C2—Investment 2.1 Enhancement and strengthening of biomedical research in the NHS.

Author contributions

M.M.: Conceptualisation; Methodology; Software; Validation; Formal analysis; Investigation; Data Curation; Writing - Original Draft; Visualisation. S.S.: Software; Formal Analysis; Investigation; Writing - Review & Editing. I.H.: Formal Analysis; Investigation; Writing - Review & Editing. C.V.: Formal Analysis; Investigation; Writing - Review & Editing. C.P.: Software; Formal Analysis; Investigation; Writing - Review & Editing. S.vd.G., R.Z., N.A.vd.G., C.F.E.H., J.B., M.C.J., J.F.B., and P.C.: Writing - Review & Editing. I.U.I.: Conceptualisation; Methodology; Writing - Review & Editing; Supervision. E.M.M.: Conceptualisation; Methodology; Software; Formal Analysis; Investigation; Writing – Review & Editing; Visualisation; Supervision. M.F.C.: Conceptualisation; Methodology; Formal Analysis; Investigation; Writing – Review & Editing; Visualisation; Supervision.

Competing interests

M.F.C. is an independent consultant for research and educational issues of Medtronic and Boston Scientific (all fees to institution), is an independent consultant for research by INBRAIN (all fees to institution), and received speaking fees for: ECMT (CME activity). CP received research fundings from Medtronic for a project unrelated to the current study. IUI is a Newronika S.p.A. consultant and shareholder. IUI received lecture honoraria and research fundings from Medtronic Inc., Newronika S.p.A. and Boston Scientific. IUI is Adjunct Professor at the Department of Neurology, NYU Grossman School of Medicine. JFB received speaker's honoraria from Medtronic and AbbVie, unrelated to this research. J.B. is shareholder of ONWARD Medical B.V., a company developing products for stimulation of the spinal cord, not related to this research. All other authors declare that they have no known competing financial interests or personal relationships that could have appeared to influence the work reported in this paper.

Additional information

Supplementary information The online version contains supplementary material available at <https://doi.org/10.1038/s41531-025-01092-y>.

Correspondence and requests for materials should be addressed to M. Fiorella Contarino.

Reprints and permissions information is available at <http://www.nature.com/reprints>

Publisher's note Springer Nature remains neutral with regard to jurisdictional claims in published maps and institutional affiliations.

Open Access This article is licensed under a Creative Commons Attribution-NonCommercial-NoDerivatives 4.0 International License, which permits any non-commercial use, sharing, distribution and reproduction in any medium or format, as long as you give appropriate credit to the original author(s) and the source, provide a link to the Creative Commons licence, and indicate if you modified the licensed material. You do not have permission under this licence to share adapted material derived from this article or parts of it. The images or other third party material in this article are included in the article's Creative Commons licence, unless indicated otherwise in a credit line to the material. If material is not included in the article's Creative Commons licence and your intended use is not permitted by statutory regulation or exceeds the permitted use, you will need to obtain permission directly from the copyright holder. To view a copy of this licence, visit <http://creativecommons.org/licenses/by-nc-nd/4.0/>.

© The Author(s) 2025